

Magneto-transport in high g-factor, low-density two-dimensional electron systems confined in $\text{In}_{0.75}\text{Ga}_{0.25}\text{As}/\text{In}_{0.75}\text{Al}_{0.25}\text{As}$ quantum wells

W. Desrat, F. Giazotto, V. Pellegrini, and F. Beltram
NEST-INFM and Scuola Normale Superiore, Piazza dei Cavalieri 7, I-56126 Pisa, Italy

F. Capotondi,* G. Biasiol, and L. Sorba*
NEST-INFM and Laboratorio Nazionale TASC-INFM, Area Science Park, I-34012 Trieste, Italy

D.K. Maude
Grenoble High Magnetic Field Laboratory, MPI-FKF and CNRS, BP 166, 38042 Grenoble Cedex 9, France
(Dated: November 17, 2018)

We report magneto-transport measurements on high-mobility two-dimensional electron systems (2DESs) confined in $\text{In}_{0.75}\text{Ga}_{0.25}\text{As}/\text{In}_{0.75}\text{Al}_{0.25}\text{As}$ single quantum wells. Several quantum Hall states are observed in a wide range of temperatures and electron densities, the latter controlled by a gate voltage down to values of $1 \times 10^{11} \text{ cm}^{-2}$. A tilted-field configuration is used to induce Landau level crossings and magnetic transitions between quantum Hall states with different spin polarizations. A large filling factor dependent effective electronic g-factor is determined by the coincidence method and cyclotron resonance measurements. From these measurements the change in exchange-correlation energy at the magnetic transition is deduced. These results demonstrate the impact of many-body effects in tilted-field magneto-transport of high-mobility 2DESs confined in $\text{In}_{0.75}\text{Ga}_{0.25}\text{As}/\text{In}_{0.75}\text{Al}_{0.25}\text{As}$ quantum wells. The large tunability of electron density and effective g-factor, in addition, make this material system a promising candidate for the observation of a large variety of spin-related phenomena.

PACS numbers: 73.43.Qt, 73.63.Hs, 72.80.Ey

I. INTRODUCTION

A number of spintronic applications would be experimentally accessible thanks to the availability of high-mobility two-dimensional electron systems (2DESs) confined in $\text{In}_x\text{Ga}_{1-x}\text{As}$ layers with $x \geq 0.75$. This stems from three different factors. First, metallic contacts on $\text{In}_x\text{Ga}_{1-x}\text{As}$ with such high Indium concentration are characterized by the absence of a Schottky barrier at the interface. This naturally provides a highly transmissive junction paving the way to the observation of Andreev reflection phenomena in superconductor/2DES hybrid systems and their study in the regime of the quantum Hall effect [1, 2]. Second, the bare g-factor is expected to be very large. For instance the bare g-factor measured by electron spin resonance was found at around -5 in $\text{In}_{0.53}\text{Ga}_{0.47}\text{As}$ [3] while effective g-factors g^* (renormalized by electron-electron interactions) with absolute values between 14 and 28 were recently suggested from magneto-transport data [4, 5]. The large resulting Zeeman spin splitting under the application of weak magnetic fields makes this semiconductor system a promising candidate for spin-valve mesoscopic devices working at relatively high temperatures [6]. Third, the large Rashba coupling constant that characterizes asymmetric $\text{In}_x\text{Ga}_{1-x}\text{As}$ layers [7] can be used for the control

of spin-dependent transport and for the creation of spin-Hall currents [7, 8]. For all of these investigations, the combination of high-mobility and relatively low electron density is a crucial requirement as well as the gate-voltage control of the various parameters mentioned above.

In addition, these systems can be of much interest for the study of magnetic phenomena associated to the crossing of Landau levels with opposite spin polarizations. These crossings can be induced in a tilted-field configuration since the ratio between the Zeeman energy (E_Z) and the cyclotron energy (E_C) increases at larger values of the tilt angle. For a large enough tilt angle this ratio reaches unity and a crossing between Landau levels of neighboring orbital indices and opposite spins is expected. It was shown, however, that this magnetic transition occurs before the coincidence between the single-particle energy levels and is induced by exchange-correlation effects [9, 10]. These transitions are triggered by the behavior of the long wave-vector limit of the spin gap (that includes many-body contributions) and therefore can be also used to determine the exchange-enhanced electronic g-factor (g^*) [11]. In the past, the experimental investigation of this class of many-body-driven magnetic transitions was mainly carried out on high-mobility 2DESs confined in GaAs/AlGaAs heterostructures. The exploitation of heterostructures based on $\text{In}_x\text{Ga}_{1-x}\text{As}$ would allow to investigate the influence of both effective mass and g-factor. In addition, the presence of a large Rashba coupling could yield new coherent Landau level configurations close to coincidence as predicted in Refs.[12, 13]. Recent tilted-field experiments performed

*Also at Dipartimento di Fisica, Università di Modena e Reggio Emilia, I-43100 Modena, Italy

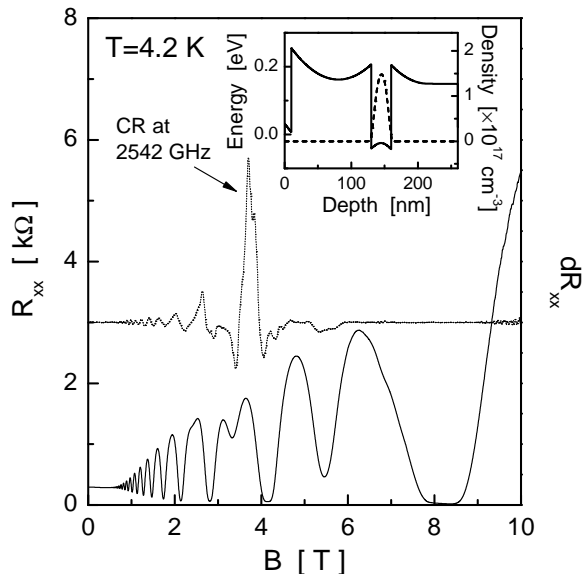


FIG. 1: Longitudinal resistance R_{xx} (solid curve, vertical left axis) and resistance change dR_{xx} (dotted curve) after far-infrared radiation at 2.542 THz as a function of magnetic field at $T = 4.2$ K. The inset shows the conduction-band diagram and charge distribution obtained from 1D Poisson-Schrödinger simulation assuming a uniform distribution of deep donor states in the barriers.

on 2DESs confined in InAs/InSb, however, showed no evidence of electron-electron interaction effects presumably due to a combination of large electron density (above 6×10^{11} cm $^{-2}$) and relatively low mobility [14].

Here we report the realization of 2DESs with mobilities well above 10^5 cm 2 /Vs confined in In $_{0.75}$ Ga $_{0.25}$ As/In $_{0.75}$ Al $_{0.25}$ As single quantum wells. These electron systems display clear quantum Hall states in a large range of temperatures and with electron densities down to $n_s = 1 \times 10^{11}$ cm $^{-2}$, the latter controlled by a gate voltage. In this paper we also report the magneto-transport analysis in a tilted magnetic-field configuration under magnetic fields up to 23 T and at millikelvin temperatures. This analysis shows crossing of spin-split Landau levels at several even-integer filling factors. These results are used to determine the exchange-enhanced "effective" electronic g-factor. Values of g^* are carefully deduced from the coincidence method with electron mass determined by cyclotron resonance and they are found to be ν -dependent. Measurements performed on a gated sample confirm this behavior for different densities. The enhanced g-factor decreases and saturates at high filling factors in agreement with the reduction of the exchange energy. From these data the change in the exchange-correlation energy at the magnetic transition between Landau states with opposite spins is also measured and is found to vary linearly as a function of the perpendicular component of the magnetic field. These results demonstrate the impact of electron-electron interactions on magnetic

transitions in In $_{0.75}$ Ga $_{0.25}$ As/In $_{0.75}$ Al $_{0.25}$ As quantum wells.

II. GATE-VOLTAGE CONTROL OF ELECTRON DENSITY

Samples analyzed in this work consist of an unintentionally doped 30 nm-wide In $_{0.75}$ Ga $_{0.25}$ As/In $_{0.75}$ Al $_{0.25}$ As quantum well metamorphically grown by molecular beam epitaxy on a (001) GaAs substrate. An In $_x$ Al $_{1-x}$ As step graded buffer with x ranging from 0.15 to 0.85 was inserted between the substrate and the 2DES to achieve almost complete strain relaxation at the quantum-well region. In these nominally undoped structures, a relatively low carrier concentration close to 3×10^{11} cm $^{-2}$ can be achieved and this confirms that there exists an intrinsic source of free carriers [15]. The origin of the doping is, however, still unclear. Preliminary results indicate the role of deep-level donor states lying in the conduction band discontinuity [16]. The inset of Fig.1 shows the conduction band diagram and the charge distribution obtained from a Poisson-Schrödinger simulation [17] assuming a uniform distribution of deep levels with activation energy of 0.12 eV. The latter was measured by photo-induced current transient spectroscopy as reported elsewhere [16]. The main panel of Fig.1 displays the longitudinal resistance R_{xx} (solid curve, vertical left axis) as a function of perpendicular magnetic field at $T = 4.2$ K. The zero-resistance regions which are well defined at even filling factors indicate the absence of parallel conduction and are associated to a quantized Hall resistance. From this data we extract a density of $n_s = 3.1 \times 10^{11}$ cm $^{-2}$ with a mobility above $\mu = 2 \times 10^5$ cm 2 /Vs (electron mean free path of the order of 1.8 μ m). Cyclotron resonance is shown on Fig.1 (dotted curve, right vertical axis) and manifests as a peak in the longitudinal resistance change dR_{xx} after far-infrared radiation at 2.542 THz as a function of magnetic field. The absorption peak is observed at $B = 3.57$ T which yields the effective mass of the conduction electrons equal to $m^* = 0.039 \pm 0.002 m_0$, where m_0 is the free electron mass.

The impact of the large g-factor and low electron mass that distinguishes this system from 2DESs confined in GaAs quantum wells is further shown in the temperature-dependent magneto-transport data displayed in Fig.2(a). The data demonstrates, in particular, that the odd-integer quantum Hall minima at $\nu = 3$ and 5 associated to the Landau level spin gap are observable at $T = 4.2$ K (up to $T \approx 11$ K for the $\nu = 3$ state) indicating the presence of robust spin-polarization at relatively low magnetic fields. An important aspect for spintronic applications in this material system stems from the possibility to reach low electron density and to control the asymmetry of the confining potential (i.e. Rashba coupling as shown in Ref.[15]) still maintaining large values of the electron mobility. In this case several recently predicted spin-related phenomena can be studied. These

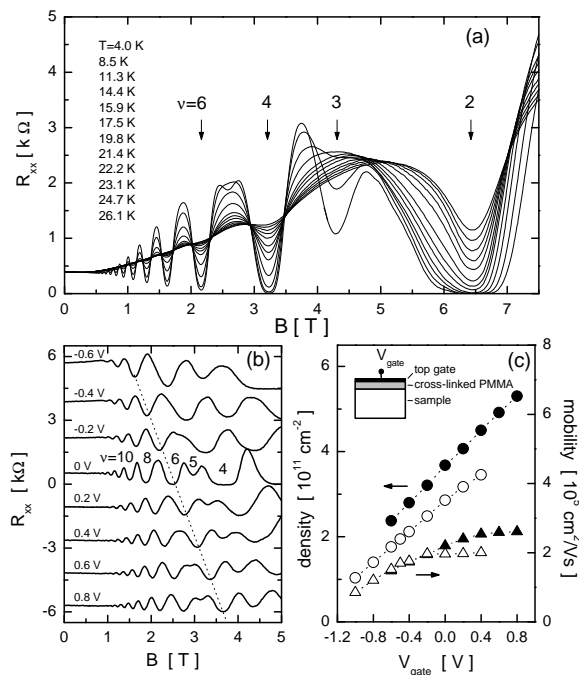


FIG. 2: (a) Longitudinal resistance R_{xx} versus magnetic field B as a function of temperature. Data correspond to sample with electron density $n_s = 3.1 \times 10^{11} \text{ cm}^{-2}$ and mobility $\mu = 2.1 \times 10^5 \text{ cm}^2/\text{Vs}$. (b) R_{xx} versus magnetic field for different values of the gate voltage V_{gate} at $T = 360 \text{ mK}$. (c) Gate voltage dependence of electron density (left vertical axis) and mobility (right vertical axis) for two different samples at $T = 360 \text{ mK}$. The sketch of the sample with gate is shown in the upper part of the panel.

include the generation of an intrinsic spin-Hall current and the control of its value for densities typically below $n_s = 1 - 1.5 \times 10^{11} \text{ cm}^{-2}$ [8]. Such low densities and their gate voltage control have never been observed in high-mobility 2DEs confined in InGaAs quantum wells with very large In concentration. Figures 2(b) and (c) demonstrate the successful achievement of these desired properties. The gate voltage control of the electron density is obtained by the application of a voltage difference between a top Ti/Au gate deposited onto a cross-linked PMMA thin layer (thickness of the order of 50 nm) and the substrate. Figure 2(b), in particular, reports the longitudinal resistivities without any parallel conduction at $T = 4.2 \text{ K}$ as a function of the gate voltage while Fig.2(c) displays the density n_s (left axis) and mobility μ (right axis) as a function of gate voltage for two different devices. A good control on the value of n_s down to a value of $1 \times 10^{11} \text{ cm}^{-2}$ can be obtained despite the uniform distribution of doping states and without altering significantly the electron mobility.

It must be noted, in addition, that the generated electric field introduces an asymmetry in the confining potential thus enhancing the value of the Rashba coupling [7]. In this relatively low-density $\text{In}_{0.75}\text{Ga}_{0.25}\text{As}$ quantum well only a limited number of Shubnikov-de Haas oscilla-

tions are detected at relatively low magnetic fields which inhibits the conventional determination of the Rashba coupling constant of the heterostructure. Previous studies, in fact, were conducted on samples having densities approaching $1 \times 10^{12} \text{ cm}^{-2}$ or above [7, 15, 18]. It can be noted in Fig.2(b), however, that an anomalous behavior characterizes the longitudinal resistance close to filling factor $\nu = 4$. The $\nu = 4$ minimum, in fact, tends to disappear at positive non-zero values of the gate voltage and this might be interpreted as precursor of the beating pattern associated to the enhancement of the Rashba coupling for a large quantum well asymmetry generated by the gate voltage [15, 18]. The analysis of the transverse resistance (data not shown) also strongly suggests a significant Rashba coupling consistent with the theoretical prediction of Ref.[19].

III. ENHANCED G-FACTOR AND MAGNETIC TRANSITIONS IN TILTED FIELDS

Having demonstrated good magneto-transport properties and their gate-voltage control we now turn to the study of the evolution of the magneto-transport in a tilted-field configuration at ultra-low temperatures. As shown below these data allow to determine the effective (exchange-enhanced) g-factor and to identify the impact of many-body effects on the magnetic transitions induced by the tilted field. For these measurements the sample was mounted on a rotation probe and placed in the mixing chamber of a dilution fridge. The maximum available magnetic field is 23 T and the bath temperature is 30 mK. The longitudinal and Hall resistances are measured on a Hall bar via a lock-in setup with a low ac current ($I = 20 \text{ nA}$, $f = 17 \text{ Hz}$). Figure 3(a) shows a waterfall graph of the longitudinal resistance R_{xx} as a function of the perpendicular magnetic field for different tilt angles θ (see inset of Fig.3(a)) at $T = 30 \text{ mK}$. At such low temperatures and at $\theta = 0^\circ$ several dissipationless QH regions at both even and odd filling factors are clearly seen from $\nu = 1$ (not shown) up to the filling factor $\nu = 12$. As the tilt angle increases, the width of these zero-resistance regions decreases for even-integer filling factors ($\nu = 4, 6, 8, 10, 12$) and increases for odd-integer filling factors ($\nu = 3, 5, 7$). This behavior is in agreement with the evolution of the respective energy gaps in the density of states as a function of θ linked to the increase of the ratio E_Z/E_C . For angles larger than 81° , however, the inverse dependence takes place, i.e. the even filling factor gaps become larger and those at odd fillings are reduced. For intermediate tilt angles, the zero-resistance region corresponding to odd-integer filling factors ($\nu = 5, 7$) saturates to its maximum width while the R_{xx} minima of the even-integer filling factors disappear and are replaced by maxima. This behavior signals the transition between QH phases with different spin polarizations and can be used to determine g^* .

Figure 3(b) displays the perpendicular magnetic field

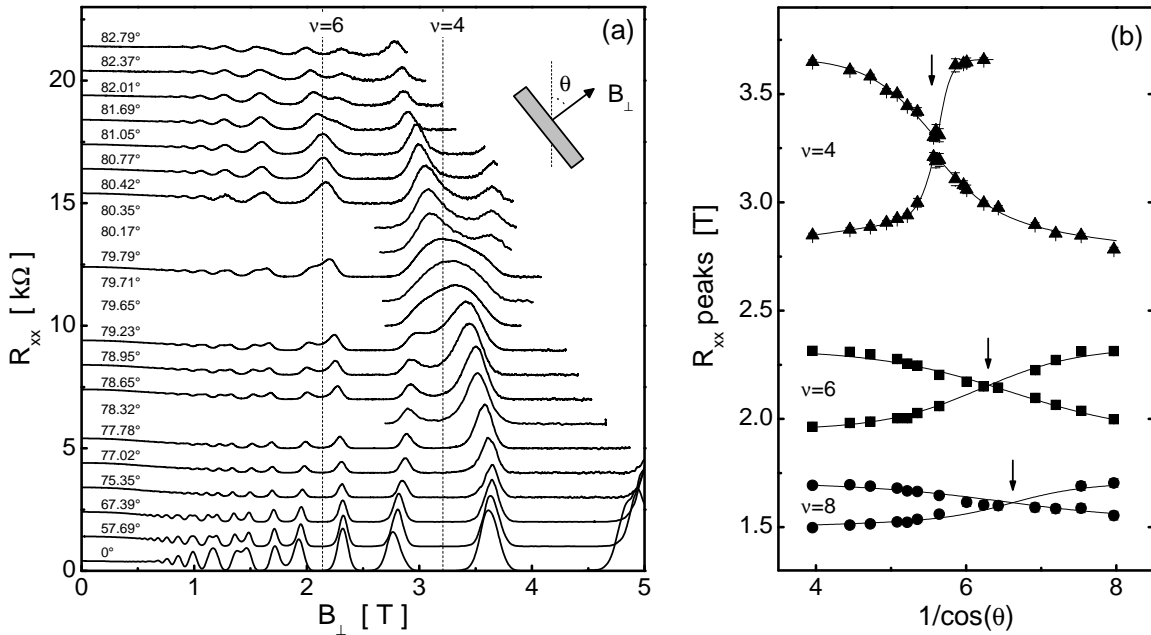


FIG. 3: (a) Perpendicular magnetic field dependence of the longitudinal resistance for different tilt angles θ . The latter were accurately obtained from the Hall voltage. The curves are shifted for clarity; the inset shows a sketch of the tilted-field geometry. (b) Perpendicular magnetic field position of the R_{xx} peaks vs $1/\cos(\theta)$. The thin lines are guides for the eye; the arrows indicate the angles ($\theta = 79.68^\circ$, 80.89° and 81.67°) at which the first coincidence of Landau levels occurs at even-integer filling factors ($\nu = 4, 6$ and 8 respectively).

position of the R_{xx} peaks of the Shubnikov-de Haas oscillations as a function of the inverse cosine of the tilt angle θ . These peak positions were estimated from the derivative curves dR_{xx}/dB . Coincidences between spin-split Landau levels, indicated by arrows, occur at different values of $1/\cos\theta_c$ (5.58, 6.32 and 6.62) for different even-integer filling factors ($\nu = 4, 6$ and 8 respectively). Using these coincidence angles and the measured effective mass, we can determine the exchange-enhanced g-factor $|g^*| = 2m_0 \cos(\theta_c)/m^*$ [11]. We obtain $|g^*| = 9.2, 8.1, 7.7$ for $\nu = 4, 6, 8$, respectively. The reduction of $|g^*|$ for larger filling factors was already reported in other material systems and is interpreted as due to the reduction of electron-electron interaction effects [20].

A similar tilted-field experiment was performed on a second $\text{In}_{0.75}\text{Ga}_{0.25}\text{As}/\text{In}_{0.75}\text{Al}_{0.25}\text{As}$ quantum well with a density of $n_s = 3.7 \times 10^{11} \text{ cm}^{-2}$ and a mobility of $\mu = 7.5 \text{ m}^2/\text{Vs}$ measured at $T = 1.4 \text{ K}$. A gate on top of this second sample allows to vary the electron density. Figure 4 shows the perpendicular magnetic field position of the R_{xx} peaks as a function of the inverse cosine of the tilt angle for three different gate voltages. The densities (mobilities) are 2.55 (5.2) and 4.9 (10) at $V_g = -0.5 \text{ V}$ and $V_g = +0.5 \text{ V}$ respectively, in units of 10^{11} cm^{-2} and m^2/Vs . In all these configurations the magnetic transitions between Landau levels with opposite spins occur at different tilt angles for different even filling factors thus confirming the impact of the many-body corrections in the material system here of interest.

The observed coincidence angles yield values for the

enhanced g-factors plotted on Fig.5 as a function of the perpendicular component of the magnetic field B_\perp . The enhanced g-factor decreases for lower perpendicular magnetic field (or higher filling factors) and lower mobilities. Having in mind that the long wavevector limit of the spin gap (relevant in magneto-transport) is the sum of the bare Zeeman energy $g_0\mu_B B$ and the exchange energy proportional to $e^2/4\pi\epsilon\ell_B$, it is tempting to describe the behavior of $g^*(B_\perp)$ by a $\sqrt{B_\perp}$ dependence. However, effects associated to mixing of Landau levels, disorder, finite-layer thickness and Coulomb correlation among electrons could play a role especially in the limit of low density. The behavior shown in Fig.5 in fact, shows a linear rather than a square root dependence on B_\perp . Additionally, the data enlighten the fact that the many-body contribution is enhanced when the mobility increases and becomes negligible at high filling factors when the enhanced g-factor saturates to the bare g-factor g_0 , which is estimated of the order of 5.5 (in absolute value). We note that the estimated value of g_0 is small compared to the theoretical one of bulk $\text{In}_{0.75}\text{Ga}_{0.25}\text{As}$ equal to $|g_0| = 8.9$. However, several recent papers also reported g-factor values strongly reduced compared to the theoretical ones. For instance, bare g-factors of -13, -8.7 or -6 have been reported in InAs quantum wells [14, 21, 22] which are far from the bulk value of around -15. It must be stressed that in the present experiments the orbital effect of the in-plane field becomes important at large tilt angles and may contribute to the reduction of g^* . It is well known, in fact, that the measurement of

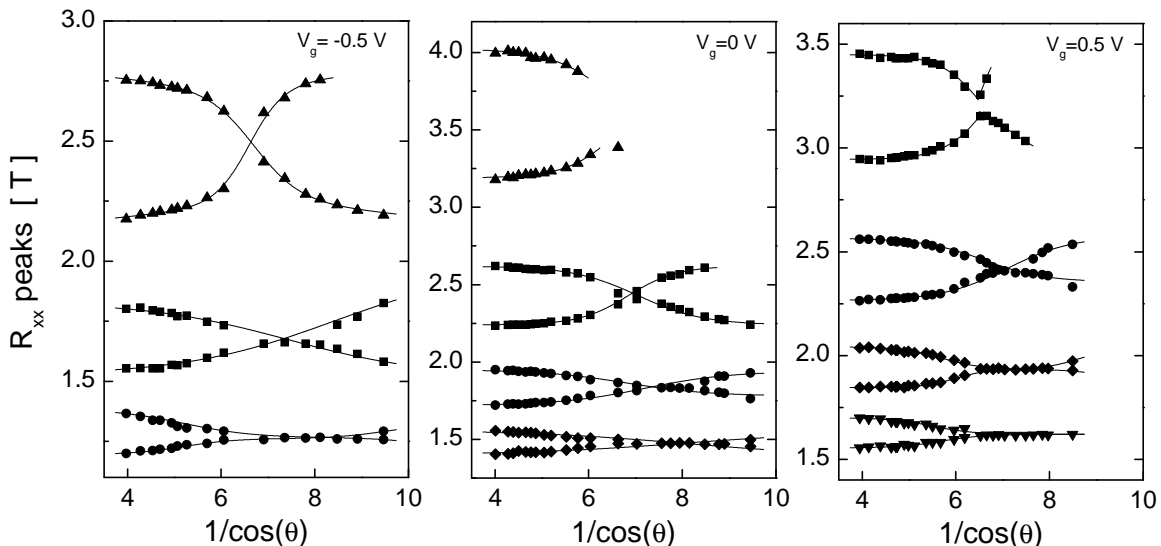


FIG. 4: Perpendicular magnetic field position of the R_{xx} peaks as a function of $1/\cos(\theta)$ for a $\text{In}_{0.75}\text{Ga}_{0.25}\text{As}/\text{In}_{0.75}\text{Al}_{0.25}\text{As}$ quantum well with a density of $n_s = 3.7 \times 10^{11} \text{ cm}^{-2}$ and a mobility of $\mu = 7.5 \times 10^4 \text{ cm}^2/\text{Vs}$. The graphs (from left to right) have been obtained at three different gate voltages : $V_g = -0.5 \text{ V}$, 0 V and $+0.5 \text{ V}$ respectively. Here data is presented for filling factors $\nu = 4$ (up triangles), 6 (squares), 8 (disks), 10 (diamonds) and 12 (down triangles). The thin lines are guides for the eye.

the electronic enhanced g-factor, and consequently of the bare g-factor, from magneto-transport measurements is not straightforward as it depends on the polarization of the system, in other words on the position of the Fermi energy in the density of states [23].

Now, with the value of the bare g-factor of $|g_0| = 5.5$, it is possible to compute the energy difference, $\hbar\omega_c/m^* - g_0\mu_B B_\perp/\cos(\theta_c)$, for all the tilt angles θ_c at which the transition is observed. This is performed for all filling factors and all gate voltages. In the single-electron picture, this difference should be equal to zero, as the first transition between neighboring Landau levels occurs when the cyclotron and Zeeman energies are equal. Due to electron-electron interactions this energy difference is finite as shown in the inset of Fig.5 as a function of the perpendicular magnetic field. These values represent the gain in the exchange-correlation energy as the system jumps from spin unpolarized to a partially spin-polarized configuration. The values obtained are significantly large and comparable or even larger to values obtained in GaAs- and AlAs-based systems [24, 25]. We see that the data points, including those obtained at different gate voltages (different densities), suggest a linear dependence vs B_\perp similar to what was reported in [25] and discussed in [26]. From these data we conclude that, even for InGaAs-based systems with large In concentration, the electron-electron interaction terms play a dominant role in determining the magnetic transitions at low filling factors, unlike previous studies on InAs systems characterized by larger electron densities [14].

Finally we want to further comment on the impact of the exchange-correlation energy gap on the magnetic transition in tilted field. The behavior shown in Fig.3

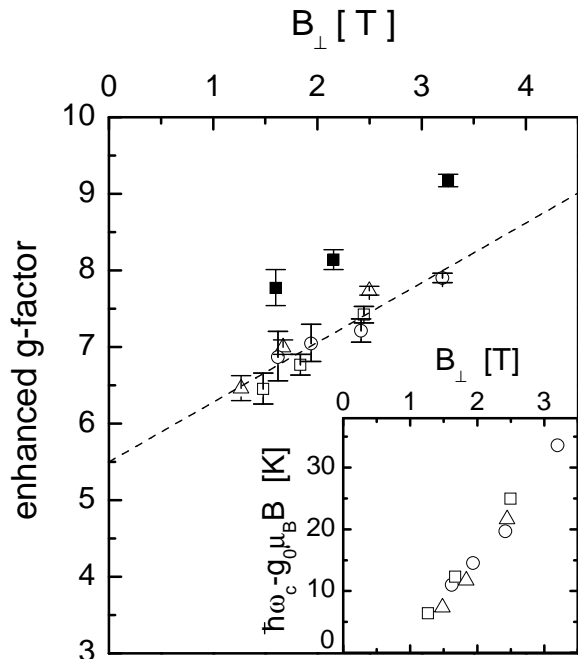


FIG. 5: Enhanced electronic g-factor (defined as $2m_0 \cos(\theta_c)/m^*$) as a function of perpendicular magnetic field for both samples presented in Fig.3b (solid squares) and Fig.4 (open symbols). The latter provides three sets of values obtained at different gate voltages : $V_g = -0.5 \text{ V}$ (open circles), $V_g = 0 \text{ V}$ (open squares) and $V_g = +0.5 \text{ V}$ (open triangles). The dashed line shows a linear dependence of g^* vs B_\perp with a zero field value equal to 5.5. In inset, energy difference, $\hbar\omega_c - g_0\mu_B B$, as a function of B_\perp .

and Fig.4 demonstrates that while a clear crossing characterizes the spin transitions at high even-integer filling factors, an anomaly in the R_{xx} peak positions close to the transition region is observed at the lower filling factors $\nu = 4$ and $\nu = 6$. We believe that this evolution signals a partial suppression of the quantum Hall gap at the transition. This is consistent with the expected first-order phase transition associated to a non-vanishing gap controlled by the exchange interaction [9]. It is also worth considering the impact of the Rashba coupling which can also lead to a repulsion of the Landau levels at crossing through the mixing of the two spin states [12, 13]. Finally it must be stressed that at the coincidence angle the magneto-resistance R_{xx} exhibits no spikes and no hysteresis at any filling factor. These effects which were reported in a number of material systems are associated to the formation of magnetic domains [25, 27, 28]. As proposed in Ref.[29], the absence of resistance spikes as well as detectable hysteresis can be explained by the presence of small and dilute magnetic domains at the transition, which in our case could be associated to fluctuations at short-length scale of the In content in the quantum well.

IV. CONCLUSION

In conclusion, we have reported the magneto-transport analysis of a 2DES confined in a

$\text{In}_{0.75}\text{Ga}_{0.25}\text{As}/\text{In}_{0.75}\text{Al}_{0.25}\text{As}$ quantum well. Several quantum Hall states were observed and the effective g-factor was measured in a tilted-field configuration. The bare g-factor was estimated of the order of $|g_0| = 5$, while the impact of electron-electron interactions was shown to play a major role at low filling factors. We have demonstrated that electron densities down to 10^{11} cm^{-2} can be achieved in nominally undoped structures by applying a gate voltage. The large measured electron mobilities at these relatively low densities make this electron system a promising candidate for those spintronics applications that would require high g-factors and gate-voltage control of the electron density. In addition, this system might be of potentially high interest for the investigation of the spin-orbit coupling and its impact on the magnetic transition of quantum Hall ferromagnetic states.

The authors are grateful to T. Jungwirth for helpful discussions and for Hartree-Fock calculations. This work was supported in part by the Ministry of University and Research (MIUR) under the FIRB "Nanotechnologies and nanodevices for the information society" and COFIN programs and by the European Research and Training Network COLLECT (Project HPRN-CT-2002-00291).

-
- [1] M. Jakob, H. Stahl, J. Knoch, J. Appenzeller, B. Lengeler, H. Hardtdegen, and H. Lüth, *Appl. Phys. Lett.* **76**, 1152 (2000).
- [2] D. Uhlisch, S. G. Lachenmann, T. Schäpers, A. I. Braginsky, H. Lüth, J. Appenzeller, A. A. Golubov, and A. V. Ustinov, *Phys. Rev. B* **61**, 12463 (2000).
- [3] M. Dobers, J. P. Vieren, Y. Guldner, P. Bove, F. Omnes, and M. Razeghi, *Phys. Rev. B* **40**, 8075 (1989).
- [4] T. Kita, Y. Sato, S. Gozu, and S. Yamada, *Physica B* **298**, 65 (2001).
- [5] Y. S. Gui, C. M. Hu, Z. H. Chen, G. Z. Zheng, S. L. Guo, J. H. Chu, J. X. Chen, and A. Z. Li, *Phys. Rev. B* **61**, 7237 (2000).
- [6] M. J. Gilbert and J. P. Bird, *Appl. Phys. Lett.* **77**, 1050 (2000).
- [7] J. Nitta, T. Akazaki, H. Takayanagi, and T. Enoki, *Phys. Rev. Lett.* **78**, 1335 (1997).
- [8] J. Sinova, D. Culcer, Q. Niu, N. A. Sinitsyn, T. Jungwirth, and A. H. MacDonald, *cond-mat/0307663* (2003).
- [9] G. F. Giuliani and J. J. Quinn, *Phys. Rev. B* **31**, 6228 (1985).
- [10] S. Koch, R. J. Haug, K. v. Klitzing, and M. Razeghi, *Phys. Rev. B* **47**, 4048 (1993).
- [11] R. J. Nicholas, R. J. Haug, K. v. Klitzing, and G. Weimann, *Phys. Rev. B* **37**, 1294 (1988).
- [12] V. I. Fal'ko, *Phys. Rev. B* **46**, 4320 (1992).
- [13] V. I. Fal'ko, *Phys. Rev. Lett.* **71**, 141 (1993).
- [14] S. Brosig, K. Ensslin, A. G. Jansen, C. Nguyen, B. Brar, M. Thomas, and H. Kroemer, *Phys. Rev. B* **61**, 13045 (2000).
- [15] T. Schäpers, G. Engels, J. Lange, T. Klocke, M. Hoffelder, and H. Lüth, *J. Appl. Phys.* **83**, 4324 (1998).
- [16] F. Capotondi, G. Biasiol, I. Vobornik, L. Sorba, F. Giazotto, A. Cavallini, and B. Fraboni, accepted in *J. Vac. Sci. Technol. B* (2003).
- [17] *1D Poisson* by G. Snider, <http://www.nd.edu/~gsnider/>.
- [18] T. Koga, J. Nitta, T. Akazaki, and H. Takayanagi, *Physica E* **13**, 542 (2002).
- [19] X. F. Wang and P. Vasilopoulos, *Phys. Rev. B* **67**, 085313 (2003).
- [20] T. Ando and Y. Uemura, *J. Phys. Soc. Jpn.* **37**, 1044 (1974).
- [21] C. M. Hu, C. Zehnder, C. Heyn, and D. Heitmann, *Phys. Rev. B* **67**, 201302 (2003).
- [22] C. H. Möller, C. Heyn, and D. Grundler, *Appl. Phys. Lett.* **83**, 2181 (2003).
- [23] R. J. Nicholas, M. A. Brummell, J. C. Portal, K. Y. Cheng, A. Y. Cho, and T. P. Pearsall, *Solid State Commun.* **45**, 911 (1983).
- [24] A. J. Daneshvar, C. J. B. Ford, M. Y. Simmons, A. V. Khaetskii, A. R. Hamilton, M. Pepper, and D. A. Ritchie, *Phys. Rev. Lett.* **79**, 4449 (1997).
- [25] E. P. D. Poortere, E. Tutuc, S. J. Papadakis, and M. Shayegan, *Science* **290**, 1546 (2000).
- [26] D. R. Leadley, R. J. Nicholas, J. J. Harris, and C. T. Foxon, *Phys. Rev. B* **58**, 13036 (1998).

- [27] V. Piazza, V. Pellegrini, F. Beltram, and W. Wegscheider, *Solid State Commun.* **127**, 163 (2003).
- [28] J. Jaroszyński, T. Andrearczyk, G. Karczewski, J. Wróbel, T. Wojtowicz, E. Papis, E. Kamińska, A. Piotrowska, D. Popović, and T. Dietl, *Phys. Rev. Lett.* **89**, 266802 (2002).
- [29] T. Jungwirth and A. H. MacDonald, *Phys. Rev. Lett.* **87**, 216801 (2001).